The Enigma of Large-Scale Permeability of Gas Shale: Pre-Existing or Frac-Induced?

Viet T. Chau[1]
Department of Civil and Environmental Engineering,
Northwestern University,
Evanston, IL 60208

Cunbao Li[1]
Department of Civil and Environmental Engineering,
Northwestern University,
Evanston, IL 60208;
Key Laboratory of Energy Engineering Safety
and Disaster Mechanics Ministry of Education,
Sichuan University,
Chengdu 610065, China;
College of Architecture and Environment,
Sichuan University,
Chengdu 610065, China

Saeed Rahimi-Aghdam[1]
Department of Civil and Environmental Engineering,
Northwestern University,
Evanston, IL 60208

Zdeněk P. Bažant[2]
McCormick Institute Professor
W.P. Murphy Professor of Civil and Mechanical
Engineering and Materials Science,
Northwestern University,
Evanston, IL 60208
e-mail: z-bazant@northwestern.edu

The existing commercial programs for simulation of hydraulic fracturing (aka fracking, or frac) of gas (or oil) shale predict parallel vertical cracks to spread in vertical parallel planes, with no lateral branching. These cracks emanate from the perforation clusters on the horizontal wellbore casing, typically spaced 10 m apart or more. For such a large spacing, the rate of gas production observed at the wellhead can be explained only upon making the hypothesis that the large-scale (or regional) permeability of shale is (even at 3 km depth) about 10,000 times higher than the gas permeability of shale measured in the lab on drilled (nondried) shale cores under confining pressures corresponding to shale at the depth of about 3 km. This hypothesis has recently been rendered doubtful by a new three-phase medium theory that takes into account the body forces due to pressure gradients of pore water diffusing into the pores. This theory predicts the fracking to produce a dense system of branched vertical hydraulic cracks with the spacing of about 0.1 m. This value matches the crack spacing deduced from the gas production rate at wellhead based on the actual lab-measured permeability. It is calculated that, to boost the permeability 10,000 times, the width of the pre-existing open (unfilled) natural cracks or joints (whose ages are distributed from one to several hundred million years) would have to be about 2.8 μm (not counting possible calcite deposits in the cracks). But this width is improbably high because, over the geologic time span, the shale must exhibit significant primary and secondary creep or flow. It is shown that the creep must close all the cracks tightly (except for residual openings of the order of 10 nm) even if the cracks are propped open by surface asperities. The inevitability of secondary creep (or steady-state flow) is explained theoretically by activation of new creep sites at stress concentrations caused by prior creep deformation. The time of transition from primary to secondary creep is taken equal to the Maxwell time estimate from geology. The overall conclusion is that the 10,000-fold increase of large-scale permeability is most likely not pre-existing but frac-induced. Although this conclusion will make little difference for long-term forecasts, it would make a major difference for the understanding and control of the frac process.
[DOI: 10.1115/1.4036455]

Introduction

Extraction of gas (or oil) from deep shale strata is made possible by hydraulic fracturing (aka fracking). The steel casing of a horizontal section of the wellbore, at the depth of about 3 km, is perforated by clusters of shaped explosive charges. The perforations provide inlets for pressurized frac water. According to computer simulations, this causes one hydraulic fracture (or frac, crack) to grow vertically from each perforation cluster. Comparisons of gas production rates for various frac spacings along the horizontal wellbore (Fig. 1) [1] indicated that the optimal spacing of these clusters (and fracs) is about 10 m (or up to 20 m).

Fracture mechanics studies show that the hydraulic cracks cannot branch. However, the 10 m spacing of the hydraulic fractures is so large that, according to the permeability values observed on slices of drilled shale cores tested in the laboratory, the gas extraction from shale would take about 100,000 years, as shown in Ref. [2]. Yet, in reality, it takes less than about 10 years.

To explain this perplexing discrepancy, it has generally been assumed that, despite the large tectonic stress in the shale stratum, there is a huge difference between the large-scale (or regional) permeability of shale and the small-scale (or local) permeability measured in the laboratory. To match the gas production rates observed at the wellhead, the large-scale permeability of shale must be assumed to be (even at a typical 3 km depth) about 10,000 times higher than the (properly measured) laboratory value (sometimes the permeability increase is said to be "only" 1000-fold or 100-fold, but this must be due to permeability testing on surface outcrops or in unrealistic conditions, e.g., without the correct triaxial confining pressures). The 10,000-fold discrepancy has been vaguely explained by pre-existing natural cracks and joints, whose typical spacing is roughly 0.1 m, and can be up to 1 m.

Here, it is argued that this explanation is dubious. The opening width of these natural cracks at the typical depth of 3 km must be zero or below 100 nm, which cannot contribute appreciably to the large-scale permeability. Rather, the explanation lies in the frac process itself, which is opening new as well as pre-existing cracks of approximately 0.1 m spacing. This process has been theoretically justified and predicted by the recently advanced three-phase medium theory [3,4].

Problematic Current Consensus

The question is whether or not large primary cracks can branch laterally, to produce hydraulic cracks of much smaller spacing. According to fracture mechanics, cracks can branch at the tip only if they propagate at a speed greater than about 40% of the Rayleigh wave speed [5,6]. But the frac process is static, as it takes one to several hours. So, crack tip branching is impossible. Indeed, all the published calculations, as well as software, based on linear or cohesive fracture mechanics or the discrete element model (DEM), predict the propagation of parallel hydraulic cracks, a single crack per perforation cluster, and no branching (Fig. 1).

[1]V. T. Chau, C. Li, and S. Rahimi-Aghdam contributed equally to this work.
[2]Corresponding author.

Contributed by the Applied Mechanics Division of ASME for publication in the Journal of Applied Mechanics. Manuscript received March 11, 2017; final manuscript received April 7, 2017; published online April 25, 2017. Editor: Yonggang Huang.

What is needed is an initiation and propagation of lateral vertical secondary cracks emanating from the walls of the primary vertical cracks, and of subsequent tertiary cracks emanating from the walls of the secondary cracks. However, according to linear elastic fracture mechanics (LEFM), no cracks can initiate from a smooth surface of the primary crack wall. Rocks, though, are quasibrittle materials, characterized by a large fracture process zone. So, one must use the cohesive (or quasibrittle) fracture mechanics, in which cracks are initiated when the material tensile strength gets exhausted. Lateral cracks in vertical planes normal to the primary vertical cracks will thus initiate if the normal stress parallel to the wall of the primary crack equals the tensile strength.

However, fluid pressure in a crack produces no tensile stresses along the crack walls (see, for example, Ref. [7]). Consequently, commercial software (marketed, e.g., by Schlumberger or NSI technologies [8,9]) predict no lateral branching of the vertical primary cracks (often simulated as narrow crack bands if the software uses the discrete element model (DEM)). Thus, in accord with the existing commercial software, the consensus has been that no secondary cracks can form, and that the only cracks created by hydraulic fracturing are those emanating from the perforation clusters on the horizontal wellbore casing, which are 10 m apart or more.

This consensus has, however, led to a dilemma: Diffusion analysis based on the values of gas permeability of shale measured in the laboratory (typically on the order of 10^{-21} m^2) [10] would predict the halftime of the history of gas production to be about 100,000 years, while the halftime of the gas production observed at the wellhead is just a few years [11]. Based on this evidence, it has been hypothesized that the large-scale permeability of shale mass ought to have a value about 10,000 times larger than the properly measured laboratory value (sometimes the increase is thought to be only 1000-fold or 100-fold, but this is likely due to oversimplified permeability testing).

As an explanation, the 10,000-fold increase of permeability has generally been attributed to the pre-existing system of natural cracks and joints. For a long time, no other explanation has been known, even though it has never been explained how at the depth of several kilometers, the natural cracks and joints in shale, tens to a few hundred million years old, could have kept their opening widths wide enough to cause such a huge permeability boost.

This general consensus has been challenged in 2016 by a new "three-phase medium" theory for hydraulic fracturing [3], which takes into account the body forces caused by gradients of the pressure of water diffusing into the pores of shale in the vicinity of primary crack walls. Some previous studies of hydraulic cracks took into account the water leak-off into the shale, but not the loading of shale by the body forces due to pore pressure gradients generated by the leak-off. It was demonstrated that a loading by these body forces (modeled in finite element analysis as applied nodal forces) can indeed create tensile stresses along the crack faces, and that these stresses can more than offset the compressive tectonic stress. This initiates lateral cohesive cracks leading eventually to a dense branched system of vertical hydraulic cracks.

The fracture evolution of the branched system, calculated according to Ref. [3], is displayed in Fig. 2. It is remarkable that the rate of opening of new cracks with a finite fracture energy and strength (on the left) is *slower by much less than an order of magnitude* in comparison to the rate of opening of pre-existing, initially perfectly closed, natural cracks with zero fracture energy and zero strength. Obviously, overcoming the confining tectonic stress at 3 km depth is far more difficult than overcoming the material strength.

The concept essential for crack branching is the *three-phase medium*, in which the first phase is the solid, the second phase is the fluid in the propagating hydraulic cracks (with progressive damage at the crack front), and the third phase is the fluid in the pores of shale. The limit cases of this medium are the Biot two-phase medium when the damage is nil, and the Terzaghi effective stress concept when the damage is complete.

Choice of Two Hypotheses

So, to explain the gas production rate at the wellhead, we must now make a choice between two hypotheses:

(1) *Hypothesis I*. There is no hydraulic crack branching (as predicted by current commercial software), but the pre-existing natural cracks and joints have, *prior to fracking*, a sufficient opening width to boost the large-scale permeability of shale mass by about four orders of magnitude.
(2) *Hypothesis II*. The pre-existing natural cracks or joints are either perfectly closed or too narrow to boost the large-scale permeability, but the *frac process opens* the pre-existing closed cracks and possibly also creates new hydraulic cracks in intact shale. This produces a dense system of branched cracks (Fig. 2) whose spacing and opening width suffice to boost the large-scale permeability by about four orders of magnitude.

Here it will be argued that the latter is far more likely. It will make a big difference for the understanding and control of the frac process, though little difference for the long-term forecasts of gas production.

Gas Permeability of Shale and Errors in Its Testing

This key property varies significantly from one shale to another. For one and the same shale, the measured permeability can vary

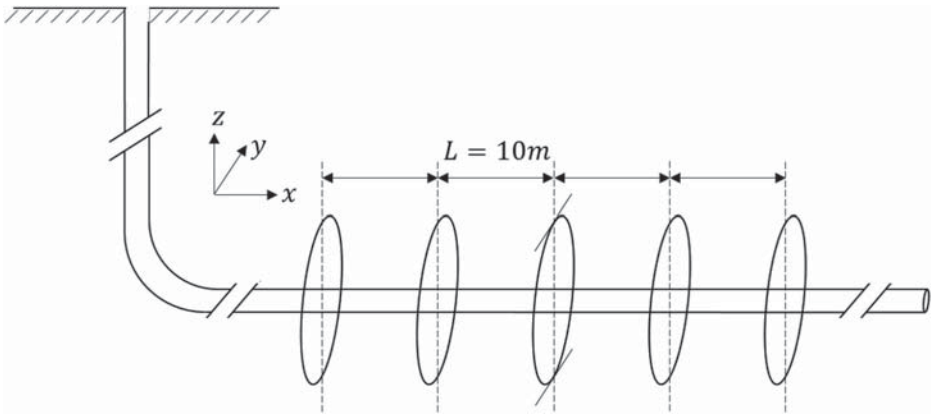

Fig. 1 Parallel hydraulic cracks as predicted in current practice (a single crack per perforation cluster, with no branching), pictured before localization [2]

even by orders of magnitude, depending on the method of measurement. Since attaining a steady state of gas flow takes a very long time, transient methods of gas permeability measurement are preferred. The pressure-decay profile method and the pulse-decay method both use a slice of a drilled core, and the third, the pressure-decay method, uses crushed rock. Regarding the first two methods, the following points should be noted:

(1) The shale is anisotropic. The gas escapes into the hydraulic cracks predominantly along the bedding planes, which are the planes of prevailing orientation of the nanoplatelets of clay minerals. The permeability in transverse direction, which is an order of magnitude lower, is, therefore, virtually irrelevant.
(2) The permeability must be measured on drilled cores extracted from the shale stratum, typically at 3 km depth (the permeability of the surface outcrops can be orders of magnitude higher).
(3) The microcracks in gas reservoirs must be closed (as argued later) because the shale has been, for tens of millions of years, under high overburden and tectonic pressures (and at temperatures around 80 °C). The test specimens should be kept at that same temperature. They must also be subjected to the same confining pressure (about 40 and 80 MPa, at the depth of about 3 km) [13], because pressure decrease is known to increase the gas permeability significantly [14–18] (by an order of magnitude for the data in Fig. 3(*a*)).
(4) Creep due to confining stress decreases the gas permeability [19] because it tends to close any flow nanochannels that may exist. Therefore, the confining stress should be applied for a long enough time (perhaps for 1 month) [17,19] (see, e.g., the data in Fig. 3(*b*)).
(5) The permeability must be measured at an unaltered moisture state, i.e., at no drying, not only because the nanopore water content greatly hinders the gas flow but also because a pore water loss causes an increase of the effective compressive stress in the solid phase, and thus a decrease of pore widths [20,21].
(6) The analysis of gas flow must take into account the slip flow, or Klinkenberg effect [22–25], in the nanopores that are not much wider than the gas adsorption layers on pore surfaces (this leads to a modified gas transport equation).

To make the tests easier, these conditions have often been disobeyed. Then the permeability of shale stratum may be overestimated by several orders of magnitude. Such simplified tests could be useful only if the ratio of conversion to the actual permeability value in the deep shale stratum were established a priori.

The measurements on crushed shale do not satisfy most of these conditions. Nevertheless, the permeability overestimation may be milder than with the other methods. The reason is that the shale gets fragmented along surfaces that pass through the largest pores, thereby eliminating these pores.

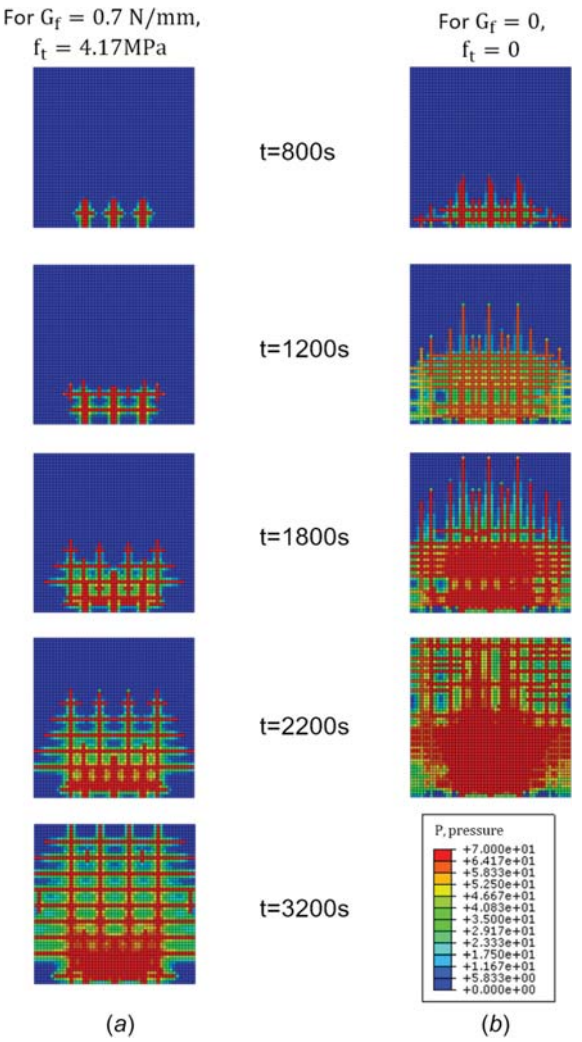

Fig. 2 Crack branching in a horizontal frac domain 5 m × 5 m simulated in Ref. [3] by three-phase medium theory with body forces due to pore pressure gradients: (*a*) for full fracture energy G_f and tensile strength f_t of crack band model [12] and (*b*) for $G_f = f_t = 0$ [3] (the horizontal wellbore lies at the bottom of each square shown, and the frac water is injected at constant pressure from three perforations clusters on the wellbore)

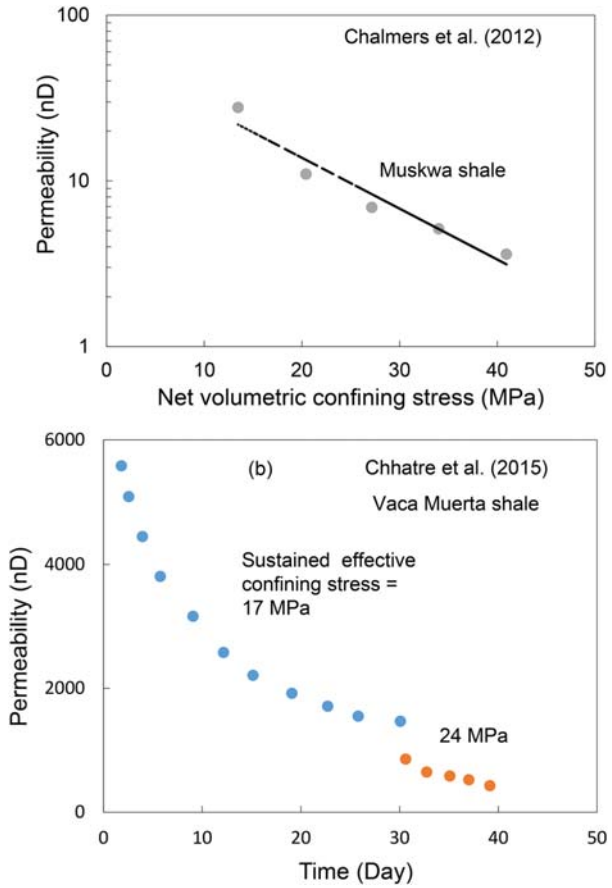

Fig. 3 Permeability of shale: (*a*) the effect of volumetric (or hydrostatic) confining stress (test data reported in Ref. [16]) and (*b*) the effect of creep (test data reported in Ref. [19])

Opening Width of Pre-Existing Natural Joints or Cracks Required by Hypothesis I

A glaring question: To boost large-scale permeability 10,000 times, what should be the opening width of the pre-existing cracks or joints? (in the case of a crack filled by calcite deposit, one must consider a crack within the calcite or a crack between the calcite and the shale wall).

To answer it, imagine an array of pre-existing planar cracks of width h and regular spacing s, parallel to the bedding planes. These cracks connect two adjacent vertical primary hydraulic cracks at distance $L = 10$ m (Fig. 4). As confirmed by the present calculations, the required crack width is expected to be big enough to make the nanoscale slip flow (or Klinkenberg effect) negligible. Then, assuming a viscous (or Poiseuille) flow of gas, we can calculate the effective permeability of the crack system, per unit cross section area of shale, as follows:

$$\kappa_h = k_t \frac{h^2}{12}\frac{h}{s} \tag{1}$$

Here, k_t (<1, assumed to be 0.5) is the tortuosity factor. It accounts for the fact the crack surface is rough and that the gas flow is obstructed by asperities or fragments bridging the crack faces.

Consider now that the permeability of intact shale, measured properly in the laboratory, is $k_1 = 10^{-6}$ mD (where mD = millidarcy $= 10^{-15}$ m^2). Then, assuming $k_t = 0.5$, the ratio $\kappa_h/\kappa_1 = 10{,}000$ is obtained for the crack width

$$h \approx 2.89\,\mu\text{m} \quad \text{if } s = 0.1\,\text{m}, \qquad h \approx 6.21\,\mu\text{m} \quad \text{if } s = 1\,\text{m} \tag{2}$$

These opening widths are 24 or 240 times bigger, respectively, than the average width of the nanopores filled by kerogen with gas.

How come that natural cracks of opening 2.89 μm or bigger are not evident in the lab, under the microscope? Doubtless it is because, during the extraction of the deep drilled core and its transfer to the surface, the cracks opened more. One of the reasons surely is the loss of confining pressure.

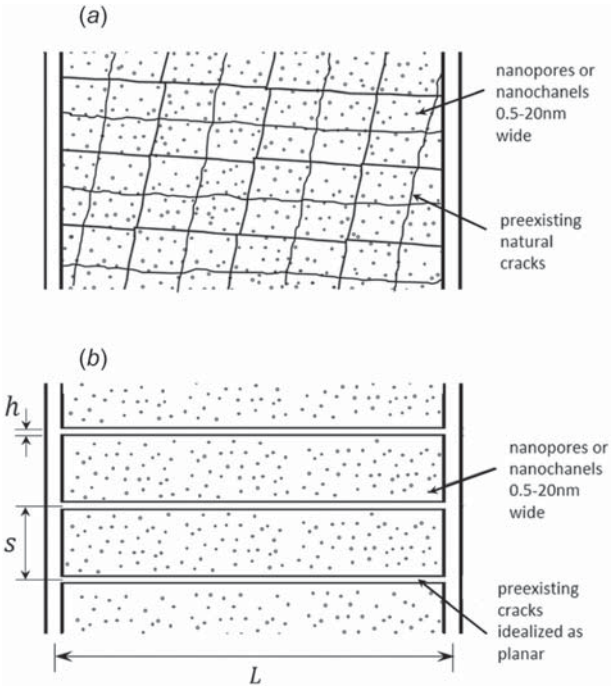

Fig. 4 Idealized array of parallel planar pre-existing natural cracks, assumed to calculate gas transport to adjacent primary hydraulic cracks spaced at $L = 10$ m

Can Gas Permeability be Inferred From Tests of Water Permeability in Deep Strata?

The "large-scale" water permeability measured in deep shale strata has been shown to be 2–4 orders of magnitude higher than the "local" water permeability measured on drilled cores in the laboratory [26–28]. The discrepancy is attributed to natural faults [29,30] and is often claimed to explain the observed 10,000-fold boost in gas permeability. However, several differences between water and gas permeability negate this claim.

(1) By contrast to small slices of intact shale in the lab, the gas in deep shale mass moves as part of a two-phase transport of gas and water. Studies of such transport in shale, as well as coal [31–35], show strong effects of viscosity, wettability, and surface slippage factor. Especially, they reveal an enormous gas permeability increase with a decreasing saturation degree (which is a behavior opposite to nanoscale water permeability). In the lab, usually the shale specimen is partially or fully dried. At depth, by contrast, the shale pores (excluding those occupied by compressed gas and organic matter, typically representing 5–20% of shale volume) are almost completely saturated by water. Its pressure equals the hydrostatic pressure for the particular depth, typically about 30 MPa (note that, as generally agreed, the pore water pressure in rock equals the hydrostatic pressure, up to the depth of at least 10 km).
(2) The drying exposure in the lab can cause the gas permeability to increase by two orders of magnitude.
(3) Transport of gas through water-filled pores is extremely slow, with effective permeability only about 10^{-25} m^2 [36–38]. While for soluble gases, the transport through water occurs by molecular diffusion, the shale gas, mostly methane, tends to form nanobubbles because it is insoluble in water. This makes the gas permeability even lower.
(4) The gas transport is further inhibited by the water blocking narrow throats on the flow passages through shale mass. The throats probably have the same width as the gas-filled pores in intact shale, which is 0.5–20 nm. Because the shale minerals are hydrophilic, part or all of the width of such throats must be filled and blocked by adsorbed water layers. How thick? Four layers on each of the opposite throat surfaces (each having one H_2O molecule thickness, 0.263 nm) is a minimal estimate (because in cement hydrates, which are more hydrophilic, the adsorbed water forms five layers at saturation) (see, for example, Ref. [39]). Thus, all the throats <2.1 nm wide are completely filled by adsorbed water, and even in throats <20 nm wide the adsorbed water plays a role. Now the point is that for gas nanobubbles, it must be next to impossible to move through the throats filled by adsorbed water layers, by displacing adsorbed water molecules which are far less mobile than free water molecules (as their lingering times attain about 10^5 periods of atomic thermal vibration).
(5) The confining pressure, too, suppresses the gas phase permeability, and does so by several orders of magnitude [35] (although the absolute permeability suppression is several times less, due to the high compressibility of gas). To compare the permeabilities κ_{rl} and κ_{rg} of the liquid and gas phases, it is found [40] that, approximately, $\kappa_{rl} \propto S^n$ and $\kappa_{rg} \propto (1-S)^n$ where S = saturation degree.
(6) One more effect complicating the permeability measurements is the swelling of shale (and pores) caused by water imbibition [41]. This phenomenon may increase water permeability.

To conclude, the answer to the question posed in the heading must be *no*.

Age of Pre-Existing Natural Fractures

To decide whether the natural cracks or joints, after being formed in some tectonic upheavals, could have remained open up to now, we must consider their age. The age of various deep shale strata varies between 100 and 300 million years. The natural fractures seen in the shale surely did not form during the last century. They must have been opened (or reopened) by various seismic or tectonic upheavals occurring at a roughly uniform frequency over the entire age of the shale formation.

Therefore, the average age of the natural cracks and joints must be at least 50 million years. Over such a time span, the creep and flow of shale cannot be neglected.

The past tectonic upheavals doubtless produced mostly shear cracks. Due to their roughness, the slip on the cracks is accompanied by dilatancy. The dilatancy leads to interrupted openings of the shear cracks or slip planes, propped by asperities in contact with the opposite faces. The question is whether these openings can be sustained, and for how long.

Creep and Flow of Shale on the Geologic Time Scale

Although some materials, such as perfect crystals or polycrystalline metals at low enough temperatures and not too high stress, do not creep, most others do, sedimentary, metamorphic, and polycrystalline rocks included. Creep of all materials under constant stress may generally be subdivided into three phases (Fig. 5(*a*)):

(1) The primary, or transient, creep, in which the creep rate is decaying;
(2) the secondary, or steady-state, creep, also called the flow, in which the strain rate remains constant; and
(3) the tertiary creep, in which the creep accelerates and leads to failure. The tertiary creep is not a strict materials property but is intertwined with a structural failure process dependent on geometry, and is irrelevant to our problem (since the shale stratum is not about to collapse).

Considering the geologic time span, we can generally describe the total creep (transient plus flow) of the lithosphere rocks under constant stress σ by the equation

$$\epsilon(t) = \epsilon_{\text{trans}}(t) + \epsilon_{\text{flow}}(t) = \frac{\sigma}{E}\left[1 + \beta\left(\frac{t}{\tau_1}\right)^n + \gamma\left(\frac{t}{\tau_2}\right)^m\right] + \xi\left(\frac{\sigma}{E}\right)^r \frac{t}{\tau_M} \tag{3}$$

in which the last term expands the equation used in Ref. [42]; ϵ = total strain, η = flow viscosity; and E, r, β, γ, ξ, n, m, τ_1,τ_2 and τ_M = material constants to be determined from laboratory tests and geologic observations (they all depend on temperature); E is the instantaneous elastic modulus (for the sake of simplicity, the shale is considered as isotropic, with E characterizing the stiffness in the vertical direction).

The first two terms, of exponents n and m, represent the primary (or transient) creep, and the last term the secondary, steady-state, creep (or flow). The linear dependence of $\epsilon(t)$ on σ in primary creep is a simplification, but probably an acceptable one (especially for the initial creep), and Boltzmann's superposition principle is approximately applicable, as widely accepted in geology for the rocks in the lithosphere [43,44].

The term with exponent n, and $\tau_1 \approx 1$ day, gives the short-term, rapidly decaying, part of transient creep (in which the number of initially activated creep sites is getting exhausted fast). According to the published creep measurements on Haynesville and Eagle Ford shales, most of which lasted only a few hours [45,46] and others only several weeks [47], the exponent, n, of the initial transient creep of shale appears to lie between 0.05 and 0.20. For $n = 0.05$, which is the value observed in Refs. [45–47], the initial creep is very close to the logarithmic creep, which was previously considered for the lithosphere rocks in general [42]. For Haynesville shale, recent experiments [47] of a few days in duration, furnished $n = 0.178$ (the other parameters being $E = 16.7$ GPa, $\beta = 2.48 \times 10^{-6}$ and $\tau_1 = 1$ day). Since $n = 0.05$ gives the fastest creep rate decay, this value is used here, to get a conservative, minimalist, estimate of crack closure.

Geologic evidence [42,43], based mainly on postglaciation rebound of the Earth mantle, suggests that exponent m of the second primary creep term is much higher, between 1/3 and 1/2, the former corresponding to what is known as the Andrade creep law [42,43]. Since the effective viscosity decreases with depth, the value of 1/3 seems more realistic for the upper lithosphere, and is used in the present calculations for the minimalist assessment of crack closure.

As sketched in Fig. 5(*a*), the transient (or primary) creep eventually transits to the secondary, steady-state, creep, or viscous flow, which is given by the last term in Eq. (3) having the time exponent of 1. According to the geologic literature [48–50], the stress exponent, r, in steady-state creep is between 2 and 3.

Based on geologic studies (see, for example, Ref. [44]), the transition from primary to secondary creep is doubtless gradual and is centered at a time characterized approximately by the Maxwell time, $\tau_M = \eta/E$, which represents the time at which the flow strain becomes equal to the elastic strain, σ/E. On the other hand, some laboratory studies suggest that the transition to steady-state creep may be centered at a certain fixed strain (approximately 0.01) rather than at a fixed time, τ_M, regardless of the applied constant stress [43]. Accordingly, the higher the sustained stress, the shorter would be the transient creep stage. This issue, however, is unimportant for the present conclusions.

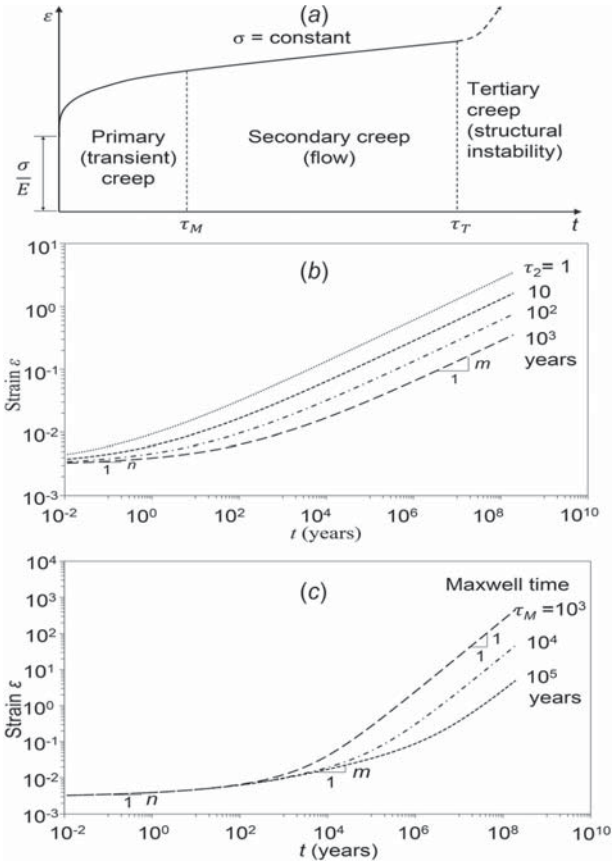

Fig. 5 (*a*) Three phases of creep evolution under constant stress, (*b*) creep evolution over 200 million years when only the primary creep terms are considered, and (*c*) the same when the secondary creep (or flow) is included

The viscosity of flow over tens of millions of years can be estimated only indirectly. Geologists estimate the average viscosity η of the Earth mantle (about 40–280 km thick) to be of the order of 10^{21} Pa·s, with the extreme estimate as high as 10^{23} Pa·s [44, pp. 198–199]. For the elastic modulus of shale, $E \approx 17.6$ GPa, this would give Maxwell time $\tau_M = \eta/E \approx 2000$–200,000 years. Since the viscosity averaging along the lithosphere includes igneous and other rocks with a much smaller creep than shale, we will consider the Maxwell time as

$$\tau_M = \frac{\eta}{E} \approx 1000 - 100,000 \quad \text{years} \tag{4}$$

The higher limit is a conservative choice for estimating the maximum possible time to crack closure.

The foregoing broad range of τ_M is here considered to compensate for various uncertainties. For example, it is hard to determine how much of the viscous resistance of the mantle is contributed by the lithosphere (i.e., the Earth crust plus asthenosphere, or the upper mantle). For processes of shorter durations, the lithosphere is in geology considered as elastic (or viscoelastic), and subject to brittle fracture, but for stresses of long enough durations, it surely exhibits flow.

Along the lithosphere (consisting of the crust and upper mantle), the segments of (not too hot) crystalline (igneous) rocks would probably exhibit little creep or flow, even over a 100 million years span. Since the series coupling of various segments along the mantle implies summation of their inverse viscosities [43], the viscosity of the shale segments is doubtless much lower than the average. This means that the estimate of τ_M in Eq. (4) is probably very much on the high side.

Further, note that the temperature increase with increasing depth in the lithosphere reduces the viscosity of solid rock by about an order of magnitude. Hence, the tectonic force must be concentrated approximately in the upper layer of the lithosphere, of about 10 km in thickness. Since the viscosities are additive in parallel coupling, this again implies that the viscosity of the layer should be much higher than its average over the whole thickness of the lithosphere.

In the logarithmic plot of Fig. 5(*c*), the initial primary (or viscoelastic) strain growth (i.e., the primary creep) is shown as the initial straight line of slope $n = 0.05$. This slope transits to slope $m = 0.3$ of the second part of primary creep. Then, centered at τ_M, the primary creep gradually transits to viscous flow, or secondary creep, which finally approaches a straight line of slope 1. To cover all possibilities, we consider in calculations three orders of magnitude of *Maxwell times*

$$\tau_M = 10^3, \ 10^4, \ 10^5 \ \text{years} \tag{5}$$

As for τ_2, a reasonable value should be close neither to τ_M nor to τ_1. It should be somewhere in the middle between τ_M and τ_1 in the log t scale. So, we will use

$$\tau_2 = \sqrt{\tau_M} = 10^{3/2}, \ 10^2, \ 10^{5/2} \ \text{years} \tag{6}$$

with 1000 years as the mean guess (in Fig. 5, neither the different values of τ_2 nor the two terms of primary creep are distinguished, to keep the trends uncluttered; distinguishing them would make a negligible difference).

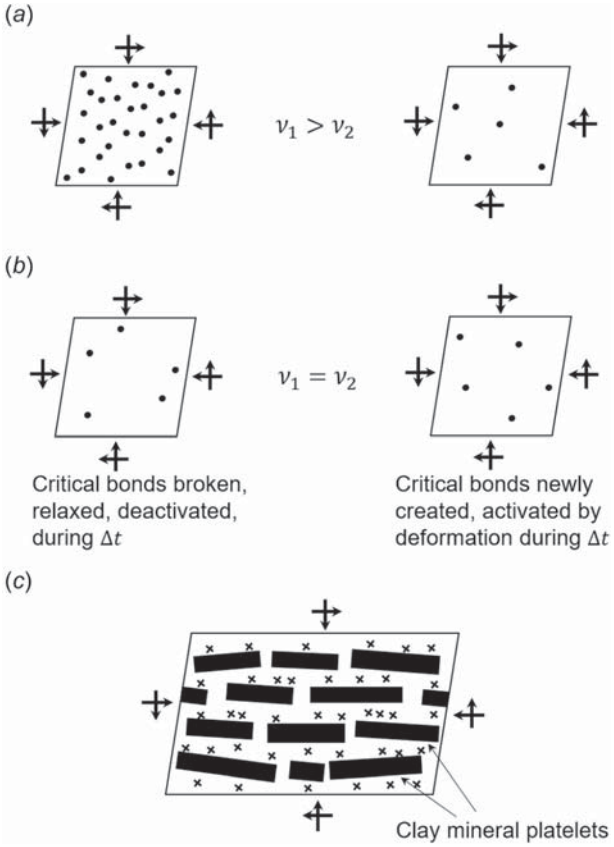

Fig. 6 Active creep sites (left) and newly created creep sites (right) of bond breakage at stress concentrations in the nanoscale of shale subjected to shear under confining pressure: (*a*) during the primary (or transient) creep, (*b*) during the secondary creep (or steady-state flow), and (*c*) creep sites (stress concentrations)

Proposed Mechanism of Shale Creep and Its Transition From Primary to Secondary Creep

The transition of primary creep to steady-state flow of shale and of other lithosphere rocks at temperatures far below melting has never been experimentally observed, and never will. So, the transition must be explained theoretically. Proposed here is a nanoscale mechanism justifying this transition.

For polycrystalline metals, specific simple examples of the atomistic creep mechanism are the Nabaro–Herring theory [51] of bulk vacancy diffusion within the crystal grains, the Coble theory of vacancy diffusion along grain boundaries, and the Harper–Dorn theory of vacancy controlled dislocation climb [52]. In shale (like in hydrated cement), the atomistic mechanism of creep is more complicated. It probably consists mainly of progressive nanoscale slips between adjacent nanoplatelets of clay minerals.

In general, the increments of creep deformation are caused by breakages and restorations of interatomic bonds at sites of high stress concentration, which may be called the creep sites (they are marked by x-points in Fig. 6, where (*a*) and (*b*) give the view normal to bedding planes, (*c*) the view across the bedding planes, with the short lines showing the clay nanoplatelets). After each slip, bond restorations must occur, or else the unloading stiffness would decrease (which would be the case of material damage rather than viscoelasticity). The breakages relax the stress concentration in the nanostructure. By transferring the applied load to nearby locations, the slips due to bond breakages must be assumed to create new creep sites of high stress concentration (Figs. 6(*a*) and 6(*b*) on the right).

In primary creep, the creep rate decays as the number, ν_1, of initially activated creep sites per unit volume of material and per unit time is gradually getting exhausted (Fig. 6). If no new creep sites with high stress concentrations were created, no creep sites would soon be left and the creep would eventually stop. This is unlikely, though.

During a creep deformation increment, the stress concentrations under constant load are getting transferred to new locations, which creates new creep sites (Figs. 6(*a*) and 6(*b*) on the right). So

$$\text{for primary creep:}\quad \nu_1 > \nu_2 > 0 \tag{7}$$

where ν_2 is the number of new creep sites created by the deformation under constant load per unit volume of material and per unit time. The difference $\nu_1 - \nu_2$ gradually decreases, which explains the increase of time exponent from n to m in Eq. (3). The primary (transient) creep eventually terminates and the secondary (steady-state) creep, or flow, begins once both numbers become equal. So

$$\text{for secondary creep:}\ \nu_1 = \nu_2 > 0 \tag{8}$$

Is the transition to secondary creep inevitable? If it did not exist, then the deformation increments would have to be creating no new creep sites, i.e., $\nu_2 = 0$. But this is improbable. If creep deformation increments under constant load create new high stress concentrations, new creep sites must form (Fig. 6). Thus, the secondary creep appears to be inevitable. The only question, yet the most difficult one, is when this transition occurs.

Closure of Open Cracks Propped by Asperities Over Geologic Times

The shale is typically intersected by systems of approximately parallel and equidistant natural cracks or joints. In surface outcrops, these cracks or joints look to be open. So, they do on the deep drilled cores brought to the surface, as the confining pressure is reduced to zero. But they were doubtless tightly closed before being cored from the deep stratum.

The spacing of natural cracks or joints varies, among different sites, from about 0.1 m to 1 m or more [53]. Let us now examine whether a pre-existing natural crack or joint could have a wide enough opening and keep it for a long enough time.

Estimate of Closing of Elliptical Channel. To this end, consider an infinite two-dimensional space in plane strain, containing an elongated elliptical hole of length $2a$ and maximum width $h = 2b$. The hole is imagined to represent the cross section of a pre-existing flow channel (Fig. 7). For simplicity of calculations, consider the shale as isotropic, with elastic modulus $E = 16.7$ GPa and Poisson ratio $\nu = 0.3$. Imposed at infinity are the horizontal principal tectonic stresses, $\sigma_h = 30$ MPa and $\sigma_H = 40$ MPa. The major axis of the ellipse is normal to the smaller tectonic stress, σ_h.

The initial elliptical hole (Fig. 7), considered to have been created tens of millions of years ago, could not have had proportions that would make it collapse immediately. We assume that $a > b$ where a and b are the major and minor axes of the ellipse (in the x and y directions, Fig. 7). Stress σ_{yy} at the sharper apex must exhaust neither the compression strength, f_c, nor the tensile strength, f_t, and the same applies to the flatter apex. According to Inglis' solution [54,55], the conditions for the stresses at the apices are

$$f_t > \sigma_{xx} = \sigma_H\left(1 + 2\frac{a}{b}\right) - \sigma_h > -f_c \tag{9}$$

$$f_t > \sigma_{yy} = -\sigma_H + \sigma_h\left(1 + 2\frac{a}{b}\right) > -f_c \tag{10}$$

where both f_t and f_c are positive, while stresses σ_{xx} and σ_{yy} are positive for tension and negative for compression.

We expect the decisive inequality to be $\sigma_{yy} > f_c$ at the sharper apex (which is checked later). Thus, we have for the aspect ratio a/b the limitation

$$\frac{a}{b} < \frac{f_c + \sigma_H - \sigma_h}{2\sigma_h} \tag{11}$$

Consider the shale to have the short-time uniaxial compression and tensile strengths $f'_c = 140$ MPa and $f'_t = 10$ MPa. For sustained loading, assume, by analogy with concrete, that the strengths for sustained long-time loading are reduced to 80% in compression and to 70% in tension, and that the biaxiality of stress (due to plane strain state) increases the strength in compression by 10% and in tension by nothing. Thus, the effective strength values to substitute into Eq. (11) are $f_c = 0.88f'_c = 123.2$ MPa and $f_t = 0.7f'_t = 7.0$ MPa. For the tectonic loading, we consider $\sigma_H = 40$ MPa and $\sigma_h = 30$ MPa (compression being positive for σ_h and σ_H). Substitution of these values into Eq. (11) yields the following maximum possible aspect ratio of the initial elliptical hole (or fluid flow conduit):

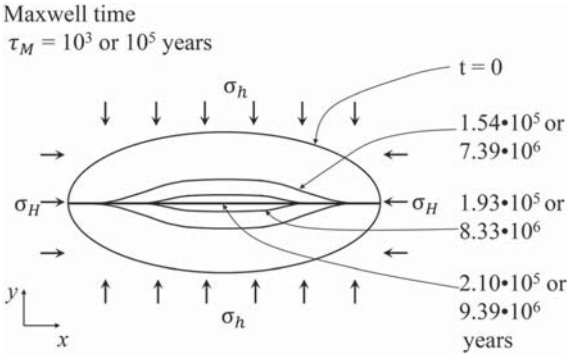

Fig. 7 Sequence of creep closure of the cross section of an elliptical channel, calculated for the expected and greatly increased values of Maxwell time τ_M of shale

$$\frac{a}{b} = 2.22 \tag{12}$$

Checking with this ratio a/b, the remaining three inequalities in Eqs. (9) and (10), one finds them satisfied.

Note that the strength limits restrict only the initial shape of the elliptical hole but not its size.

Although the initial small deflections due to elasticity and initial primary creep could be obtained analytically, we are interested in the complete closing of the hole, for which finite strains must be considered. The finite element software ABAQUS, having the facility to simulate the contact of opposite faces of the collapsing hole, has been used for this purpose.

Since, in view of all the other crude approximations, high accuracy is not needed, it suffices to treat the creep and flow deformations as the elastic deformation for effective modulus $E_{ef}(t) = 1/J(t)$ and a constant Poisson ratio, where $J(t) = \epsilon(t)/\sigma$ = compliance function of shale. For the sake of simplicity, we consider the creep to be linearly viscoelastic, defined by the compliance function based on Eq. (3) for $\sigma = \sigma_h$, i.e.,

$$J(t) = \frac{1}{E}\left[1 + \beta\left(\frac{t}{\tau_1}\right)^n + \gamma\left(\frac{t}{\tau_2}\right)^m\right] + \xi\frac{\sigma_h{}^{r-1}}{E^r}\frac{t}{\tau_M} \tag{13}$$

where $\beta = 2.48 \times 10^{-6}$, $\tau_1 = 1$ day, $\gamma = 1.0 \times 10^{-5}$, $\xi = 0.5$, and $r = 2.5$.

The computed subsequent profiles of the closing of the elliptical hole (or conduit) are plotted in Fig. 7. Since the profile evolutions for different τ_M values are similar, only one figure suffices. The times to reach each profile are in the figure indicated for $\tau_M = 1000$ days and 100,000 days. The times, t_c, for the hole to close completely are obtained as

$$\begin{aligned}&\text{for } \tau_M = 10^3 \text{ years:}\quad t_c = 2.10 \times 10^5 \text{ years}\\ &\text{for } \tau_M = 10^5 \text{ years:}\quad t_c = 9.36 \times 10^6 \text{ years}\quad \text{(upper bounds)}\end{aligned} \tag{14}$$

These time estimates represent upper bounds. In reality, the times to close the hole would be much shorter because we

neglected the increased flow due to stress concentrations near the ellipse surface, especially near the sharper apex (where $\sigma_{yy} = 123\,\text{MPa} = 4.11\sigma_h$). These concentrations would make the nonlinear flow term much greater, and thus the times to closing much shorter (according to the assumed creep law). However, an accurate calculation of creep closing times is not important because even the upper bounds in Eq. (14) represent small fractions of the average age of natural cracks in the shale stratum (>50 million years).

Estimate of Closing of Propped Flat Crack. Another case that can be easily calculated is a flat open crack of a large extent propped by surface asperities, formed during its creation by some seismic event in the distant past. To allow simple calculation, consider the two-dimensional plane-strain problem of an infinite initial crack of width h_c in an infinite plane, propped at intervals L_g by pillar walls of width L_p; see Fig. 8. The shale properties are the same as before.

The pillar walls are subjected to the average compression stress σ_p much higher than σ_h. Therefore, a compliance function with a greater flow term is considered for the pillar walls

$$J(t) = \frac{1}{E}\left[1 + \beta\left(\frac{t}{\tau_1}\right)^n + \gamma\left(\frac{t}{\tau_2}\right)^m\right] + \xi\frac{{\sigma_p}^{r-1}}{E^r}\frac{t}{\tau_M}, \qquad \sigma_p = \sigma_h\frac{L_g}{L_p} \tag{15}$$

while $J(t)$ according to Eq. (13) is considered for all the rest, i.e., the increased flow due to the stress concentrations near the corners is neglected, which causes the closing times estimate to be an upper bound. The maximum possible ratio L_g/L_p is such that the pillar wall is at the limit of crushing, i.e., the stress in the pillar walls would not exceed the compression strength f_c. This condition yields $L_g/L_p = 4$.

The ABAQUS finite element program with finite strain and a contact algorithm was used to calculate the progressive closing of the cracks; see Fig. 8, which also gives the times to reach subsequent closure states for the expected and extreme estimates of τ_M. The times needed for a virtually complete closure are

$$\begin{aligned} &\text{for } \tau_M = 10^3 \text{ years}: \quad t_c = 5500 \text{ years} \\ &\text{for } \tau_M = 10^5 \text{ years}: \quad t_c = 35,600 \text{ years (upper bounds)} \end{aligned} \tag{16}$$

Again, it is found that the pillar walls, simulating crack surface asperities, cannot prevent crack closure over a time period that would matter.

In summary, although the existence of a steady-state flow of shale over a 100 million year time span is, and will remain, unproven by direct observations, it must logically be expected—based on analysis of various geological observations, on analogies with many other materials, and on micromechanical considerations. It would be farfetched to assume the pre-existing natural cracks and joints in shale to have, at 3 km depth, a width sufficient to enhance the large-scale gas permeability appreciably.

Minimum Pore or Crack Width at Nanoscale

It should be pointed out, though, that there exists a certain maximum nanoscale opening width of natural cracks that can be sustained even over tens of millions of years. This is demonstrated by the fact that the pores and channels filled by kerogen and gas have a finite width, distributed between 0.5 nm and about 20 nm, with 7 nm as the average.

Why do they not close?–Because the closure is resisted by development of high pressure in the entrapped kerogen and gas, equal to the tectonic stress (to realize the magnitudes, note that, according to the ideal gas equation, the pressure in a spherical gas-filled pore of diameter 100 nm increases from the atmospheric pressure of 0.1 MPa to 40 MPa if the diameter is reduced to 13.6 nm).

The gas-filled nanopores or nanochannels, representing 5–20% of volume in various types of gas shale, are the source of the local permeability of shale. This permeability suffices to explain the observed gas output when the hydraulic cracks are considered to be roughly 0.1 m apart [2]. But such nanochannels can make virtually no contribution to the gas output when the hydraulic cracks are assumed to be 10 m apart.

Sealing of Pre-Existing Natural Cracks by Calcite

Independently of the foregoing creep analysis, one other phenomenon, which alone suffices to render Hypothesis I dubious, is the tight filling of open cracks by calcite [53,56,57]. When the drilled cores are brought to the surface, the natural cracks or joints might seem not be filled by calcite tightly. But, under the confining pressures in deep shale strata, they probably are, and thus cannot increase the large-scale gas permeability.

In geologic history, the filling by calcite must have been completed before the cracks, freshly created by some tectonic event, could have been closed by creep. It follows that the time needed for the tight filling of natural cracks by calcite is negligible compared to the average age of natural cracks.

Note: Before closing, we may digress to granite. Aside from instability of parallel crack systems, the lack of sufficient porosity and pore connectivity now appears to be another reason why a branched hydraulic crack system could not be produced in hot granite, as a means to harness geothermal energy for generating electricity [58–60]. But it should work if the hot rock is sufficiently porous.

Conclusions

(1) *Hypothesis I*, which posits that pre-existing natural cracks and joints boost the large-scale permeability of shale by about 4 orders of magnitude compared to the permeability measured on deep drilled cores, is not the only way to explain the observed gas production history from wells in which the spacing of perforation clusters is about 10 m.
(2) Recently, an alternative explanation, *Hypothesis II*, emerged. It is based on the recent development of a three-phase medium theory for hydraulic fracturing. This theory, which takes into account the body forces due to pressure gradients of pore water diffusing (or leaking) from the primary hydraulic cracks into the shale, predicts the development of a branched system of vertical hydraulic cracks with the spacing of about 0.1 m. With such a crack spacing, the observed gas production rate can be explained without postulating any huge large-scale permeability enhancement.
(3) Hypothesis I is predicated on assuming the pre-existing natural cracks or joints to be empty and have an opening width of at least 2.8 μm. A much bigger width would be necessary if these cracks or joints were perfectly saturated by water.
(4) Opening widths > 2.8 nm are highly improbable because, over the span of 100 million years or more, the shale most likely exhibits secondary creep or flow. This flow would have had to close the cracks tightly (except the cracks less than about 100 nm wide which, however, cannot have an appreciable effect on the rate of gas production from primary hydraulic cracks spaced about 10 m apart).
(5) Because of primary and secondary creep, a flow channel in shale, with a cross section approximated as an ellipse, must get closed in much less than within mere 210,000 years for the expected Maxwell time and within 9,390,000 years for the extreme estimate of Maxwell time. For a flat crack propped by rectangular pillar walls, the corresponding closure times are 5500 years 256,000 years, respectively (due to simplifications of analysis, all these times are mathematically upper bounds, in view of the assumptions made).

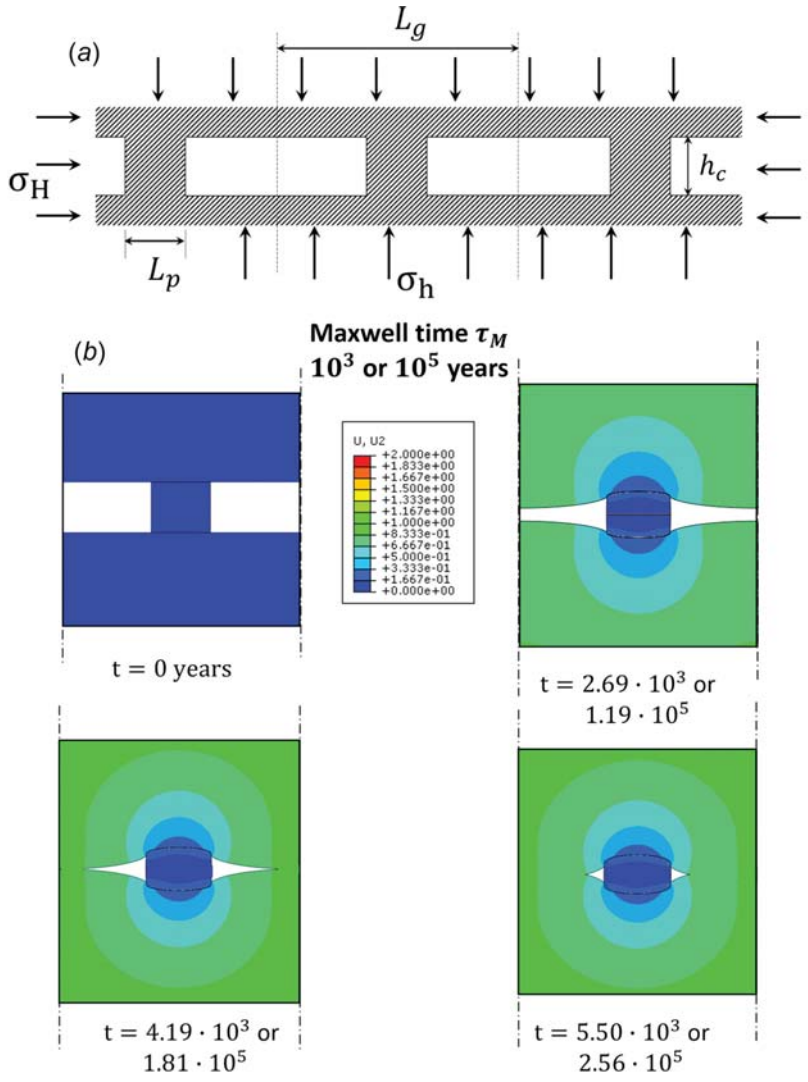

Fig. 8 (*a*) Idealization of planar crack in shale kept open by asperities imagined as rectangular pillar walls and (*b*) subsequent states of creep closure for the expected and greatly increased values of Maxwell time τ_M of shale

(6) The existence of secondary creep in shale or other rocks over geologic time span appears necessary if one realizes that every increment of creep deformation must not only deactivate some creep sites but also activate new ones. Denying it would be tantamount to a denial of activation of new creep sites.
(7) It appears that the time of transition to secondary creep, or steady-state flow, can be roughly estimated as the Maxwell time. Its value may be inferred from the viscosity indicated by geologic models for the history of the upper layer of Earth lithosphere.
(8) If a fresh natural crack created by a tectonic upheaval is getting filled by calcite, the time to tight filling must be much shorter than the time to close the cracks by creep.
(9) Pre-existing or frac-induced?—Most likely frac-induced.

Closing comment: Resolving the present questions is necessary to enable a rational control of the frac process.

Acknowledgment

Partial financial support from the U.S. Department of Energy through Subcontract No. 37008 of Northwestern University with Los Alamos National Laboratory is gratefully acknowledged. The simulation of fracturing damage received also some support from ARO Grant No. W911NF-15-101240 to Northwestern University. The first author wishes to thank the Department of Science and Technology of Sichuan Province (Nos. 2015JY0280 and 2012FZ0124), NSFC (No. 41472271) and CSC for supporting him as a Visiting Predoctoral Research Fellow at Northwestern University. Furthermore, Giuseppe Buscarnera, James P. Hambleton, William Carey, Matthew Vandamme, Andrew P. Bunger, Paulo Monteiro, Nick Barton and Mohamed Y. Soliman are thanked for valuable discussions.

Appendix: The Question of Pre-Existing Natural Cracks Permanently Filled by Water or Organic Fluids

One cannot rule out the possibility that the tectonic upheaval in distant past might have created a crack or hole that got completely filled by pressurized water before the tectonic stress could close it. If the water pressure equaled the tectonic stress, creep closing of the crack would be prevented. However, one may note two objections: (1) Could such a water-filled pressurized crack avoid getting filled by calcite? and (2) could it provide effective transport of

shale gas from the nanopores to the primary hydraulic cracks spaced 10 m apart or more? Both seem very improbable, for two reasons.

First, deposition of calcite in open cracks seems to be a general feature, and incomplete filling probably exists only after the drilled core has been brought to surface. As recent scanning electron microscope (SEM) observations on fractured Barnett shale [53,56] illustrate, nearly all natural cracks are very narrow and filled by calcite completely. Those which are wider than 10 mm are rare, highly tortuous and spaced about 100 m apart, and thus could not convey much gas to primary cracks > 10 m apart.

Second, geologists know that, down to at least 10 km in depth, all cracks are saturated and, in the case of shale, contain a mixture of water and organic matter (kerogen and gas, for the most part methane). However, Hildebrand et al. [36,37] surmised that the gas permeability of such completely saturated pores (which is not the case of fresh hydraulically produced cracks) is extremely low, apparently as low as 10^{-25}m^2 (or about 10^{-10} mD). In that case, the contribution to the gas production rate would be negligible. It would be hard to explain the relatively fast transport of gas through the new hydraulic cracks toward the well casing.

References

[1] Soliman, M., and Grieser, W., 2010, "Analyzing, Optimizing Frac Treatments by Means of a Numerical Simulator," J. Pet. Technnol., **62**(7), pp. 22–24.
[2] Bažant, Z. P., Salviato, M., Chau, V. T., Viswanathan, H., and Zubelewicz, A., 2014, "Why Fracking Works," ASME J. Appl. Mech., **81**(10), p. 101010.
[3] Chau, V. T., Bažant, Z. P., and Su, Y., 2016, "Growth Model for Large Branched Three-Dimensional Hydraulic Crack System in Gas or Oil Shale," Philos. Trans. R. Soc., A, **374**(2078), p. 20150418.
[4] Bažant, Z. P., and Chau, V. T., 2016, "Recent Advances in Global Fracture Mechanics of Growth of Large Hydraulic Crack Systems in Gas or Oil Shale: A Review," *New Frontiers in Oil and Gas Exploration*, C. Jin, and G. Cusatis, eds., Springer International Publishing, Cham, Switzerland, Chap. 13.
[5] Yoffe, E. H., 1951, "The Moving Griffith Crack," London, Edinburgh, Dublin Philos. Mag. J. Sci., **42**(330), pp. 739–750.
[6] Ravi-Chandar, K., and Knauss, W., 1984, "An Experimental Investigation Into Dynamic Fracture—III: On Steady-State Crack Propagation and Crack Branching," Int. J. Fract., **26**(2), pp. 141–154.
[7] Anderson, T. L., 2005, *Fracture Mechanics: Fundamentals and Applications*, CRC Press, Boca Raton, FL.
[8] Schlumberger, 2012, "FracCADE," Schlumberger, Houston, TX.
[9] NSI Technologies, 2014, "StimPlan, Version 7.0," NSI Technologies Inc., Tulsa, OK.
[10] Sakhaee-Pour, A., and Bryant, S., 2012, "Gas Permeability of Shale," SPE Reservoir Eval. Eng., **15**(4), pp. 401–409.
[11] Mason, J. E., 2011, "Well Production Profiles Assess Fayetteville Shale Gas Potential," Oil Gas J., **109**(11), p. 76.
[12] Bazant, Z. P., 1982, "Crack Band Model for Fracture of Geomaterials," Proceedings of the Fourth International Conference on Numerical Methods in Geomechanics (ICONMIG), Edmonton, Canada, May 31–June 4, pp. 1137–1152.
[13] Zoback, M. D., 2007, *Reservoir Goemechanics*, Cambridge University Press, Cambridge, UK.
[14] Kwon, O., Kronenberg, A. K., Gangi, A. F., and Johnson, B., 2001, "Permeability of Wilcox Shale and Its Effective Pressure Law," J. Geophys. Res.: Solid Earth, **106**(B9), pp. 19339–19353.
[15] Dong, J. J., Hsu, J. Y., Wu, W. J., Shimamoto, T., Hung, J. H., Yeh, E. C., and Sone, H., 2010, "Stress-Dependence of the Permeability and Porosity of Sandstone and Shale From TCDP Hole-A," Int. J. Rock Mech. Min. Sci., **47**(7), pp. 1141–1157.
[16] Chalmers, G. R., Ross, D. J., and Bustin, R. M., 2012, "Geological Controls on Matrix Permeability of Devonian Gas Shales in the Horn River and Liard Basins, Northeastern British Columbia, Canada," Int. J. Coal Geol., **103**, pp. 120–131.
[17] Cui, X., Bustin, A. M. M., and Bustin, R. M., 2009, "Measurements of Gas Permeability and Diffusivity of Tight Reservoir Rocks: Different Approaches and Their Applications," Geofluids, **9**(3), pp. 208–223.
[18] Rydzy, M. B., Patino, J., Elmetni, N., and Appel, M., 2016, "Stressed Permeability in Shales: Effects of Matrix Compressibility and Fractures—A Step Towards Measuring Matrix Permeability in Fractured Shale Samples," International Symposium of the Society of Core Analysts (SCA), Snowmass, CO, pp. 1–12.
[19] Chhatre, S. S., Braun, E. M., Sinha, S., Determan, M. D., Passey, Q. R., Zirkle, T. E., and Kudva, R. A., 2015, "Steady-State Stress-Dependent Permeability Measurements of Tight Oil-Bearing Rocks," Petrophysics, **56**(2), pp. 116–124.
[20] Ghanizadeh, A., Bhowmik, S., Haeri-Ardakani, O., Sanei, H., and Clarkson, C. R., 2015, "A Comparison of Shale Permeability Coefficients Derived Using Multiple Non-Steady-State Measurement Techniques: Examples From the Duvernay Formation, Alberta (Canada)," Fuel, **140**, pp. 371–387.
[21] Falk, K., Coasne, B., Pellenq, R., Ulm, F. J., and Bocquet, L., 2015, "Subcontinuum Mass Transport of Condensed Hydrocarbons in Nanoporous Media," Nat. Commun., **6**, p. 6949.
[22] Klinkenberg, L. J., 1941, "The Permeability of Porous Media to Liquids and Gases," American Petroleum Institute, New York, pp. 200–213.
[23] Jones, S. C., 1994, "A New, Fast, Accurate Pressure-Decay Probe Permeameter," SPE Form. Eval., **9**(3), pp. 193–199.
[24] Gensterblum, Y., Ghanizadeh, A., Cuss, R. J., Amann-Hildenbrand, A., Krooss, B. M., Clarkson, C. R., and Zoback, M. D., 2015, "Gas Transport and Storage Capacity in Shale Gas Reservoirs: A Review—Part A: Transport Processes," J. Unconv. Oil Gas Resour., **12**, pp. 87–122.
[25] Monteiro, P. J. M., Rycroft, C. H., and Barenblatt, G. I., 2012, "A Mathematical Model of Fluid and Gas Flow in Nanoporous Media," Proc. Natl. Acad. Sci., **109**(50), pp. 20309–20313.
[26] Brace, W. F., 1980, "Permeability of Crystalline and Argillaceous Rocks," Int. J. Rock Mech. Min. Sci. Geomech. Abstr., **17**(5), pp. 241–251.
[27] Brace, W. F., 1984, "Permeability of Crystalline Rocks: New in Situ Measurements," J. Geophys. Res.: Solid Earth, **89**(B6), pp. 4327–4330.
[28] Huenges, E., Erzinger, J., Keck, J., Engeser, B., and Kessels, W., 1997, "The Permeable Crust: Geohydraulic Properties Down to 9101 m Depth," J. Geophys. Res.: Solid Earth, **102**(B8), pp. 18255–18265.
[29] Townend, J., and Zoback, M. D., 2000, "How Faulting Keeps the Crust Strong," Geology, **28**(5), pp. 399–402.
[30] Zoback, M. D., and Townend, J., 2001, "Implications of Hydrostatic Pore Pressures and High Crustal Strength for the Deformation of Intraplate Lithosphere," Tectonophysics, **336**(1), pp. 19–30.
[31] Massarotto, P., 2002, "4-D Coal Permeability Under True Triaxial Stress and Constant Volume Conditions," Ph.D. thesis, The University of Queensland, Brisbane, Australia.
[32] Sereshki, F., 2005, "Improving Coal Mine Safety by Identifying Factors That Influence the Sudden Release of Gases in Outburst Prone Zones," Ph.D. thesis, University of Wollongong, New South Wales, Australia.
[33] Han, F., Busch, A., Krooss, B. M., Liu, Z., van Wageningen, N., and Yang, J., 2010, "Experimental Study on Fluid Transport Processes in the Cleat and Matrix Systems of Coal," Energy Fuel, **24**(12), pp. 6653–6661.
[34] Pan, Z., Connell, L. D., and Camilleri, M., 2010, "Laboratory Characterisation of Coal Reservoir Permeability for Primary and Enhanced Coalbed Methane Recovery," Int. J. Coal Geol., **82**(3), pp. 252–261.
[35] Ghanizadeh, A., Gasparik, M., Amann-Hildenbrand, A., Gensterblum, Y., and Krooss, B. M., 2014, "Experimental Study of Fluid Transport Processes in the Matrix System of the European Organic-Rich Shales—I: Scandinavian Alum Shale," Mar. Pet. Geol., **51**, pp. 79–99.
[36] Hildenbrand, A., Schlämer, S., and Krooss, B. M., 2002, "Gas Breakthrough Experiments on Fine-Grained Sedimentary Rocks," Geofluids, **2**(1), pp. 3–23.
[37] Hildenbrand, A., Schlämer, S., Krooss, B. M., and Littke, R., 2004, "Gas Breakthrough Experiments on Pelitic Rocks: Comparative Study With N_2, CO_2 and CH_4," Geofluids, **4**(1), pp. 61–80.
[38] Amann-Hildenbrand, A., Bertier, P., Busch, A., and Krooss, B. M., 2013, "Experimental Investigation of the Sealing Capacity of Generic Clay-Rich Caprocks," Int. J. Greenhouse Gas Control, **19**, pp. 620–641.
[39] Bažant, Z. P., 1972, "Thermodynamics of Interacting Continua With Surfaces and Creep Analysis of Concrete Structures," Nucl. Eng. Des., **20**(2), pp. 477–505.
[40] Wang, C. Y., and Beckermann, C., 1993, "A Two-Phase Mixture Model of Liquid-Gas Flow and Heat Transfer in Capillary Porous Media—I: Formulation," Int. J. Heat Mass Transfer, **36**(11), pp. 2747–2758.
[41] Schmitt, L., Forsans, T., and Santarelli, F. J., 1994, "Shale Testing and Capillary Phenomena," Int. J. Rock Mech. Min. Sci. Geomech. Abstr., **31**(5), pp. 411–427.
[42] Murrell, S. A. F., 1976, "Rheology of the Lithosphere—Experimental Indications," Tectonophysics, **36**(1–3), pp. 5–24.
[43] Birger, B. I., 2012, "Transient Creep and Convective Instability of the Lithosphere," Geophys. J. Int., **191**(3), pp. 909–922.
[44] Ranalli, G., 1987, *Rheology of the Earth*, Allen & Unwin, Boston, MA, Sec. 8.3.
[45] Sone, H., and Zoback, M. D., 2014, "Time-Dependent Deformation of Shale Gas Reservoir Rocks and Its Long-Term Effect on the In Situ State of Stress," Int. J. Rock Mech. Min. Sci., **69**, pp. 120–132.
[46] Sone, H., and Zoback, M. D., 2013, "Mechanical Properties of Shale-Gas Reservoir Rocks Part—2: Ductile Creep, Brittle Strength, and Their Relation to the Elastic Modulus," Geophysics, **78**(5), pp. D393–D402.
[47] Rassouli, F., and Zoback, M., 2016, "A Comparison of Short-Term and Long-Term Creep Experiments in Unconventional Reservoir Formations," 50th U.S. Rock Mechanics/Geomechanics Symposium, American Rock Mechanics Association, Houston, TX, June 26–29, p. ARMA-2016-430.
[48] Carter, N. L., and Ave'Lallemant, H. G., 1970, "High Temperature Flow of Dunite and Peridotite," Geol. Soc. Am. Bull., **81**(8), pp. 2181–2202.
[49] Raleigh, C. B., and Kirby, S. H., 1970, "Creep in the Upper Mantle," Mineral. Soc. Am. Spec. Pap., **3**, pp. 113–121.
[50] Murrell, S. A. F., and Chakravarty, S., 1973, "Some New Rheological Experiments on Igneous Rocks at Temperatures Up to 1120°C," Geophys. J. Int., **34**(2), pp. 211–250.
[51] Cotrell, A. H., 1964, *The Mechanical Properties of Matter*, Wiley, New York.
[52] Meyers, M. A., and Chawla, K. K., 1999, *Mechanical Behavior of Materials*, Prentice Hall, Upper Saddle River, NJ, pp. 555–557.

[53] Gale, J. F., Reed, R. M., and Holder, J., 2007, "Natural Fractures in the Barnett Shale and Their Importance for Hydraulic Fracture Treatments," AAPG Bull., **91**(4), pp. 603–622.
[54] Inglis, C. E., 1913, "Stresses in a Plate Due to the Presence of Cracks and Sharp Corners," Trans. Inst. Nav. Archit., **55**, pp. 219–230.
[55] Timoshenko, S. P., and Goodier, J. N., 1970, *Theory of Elasticity*, 3rd ed., McGraw-Hill, New York, p. 193.
[56] Gale, J. F. W., Laubach, S. E., Olson, J. E., Eichhubl, P., and Fall, A., 2014, "Natural Fractures in Shale: A Review and New Observations," AAPG Bull., **98**(11), pp. 2165–2216.
[57] Dutton, S. P., White, C. D., Willis, B. J., and Novakovic, D., 2002, "Calcite Cement Distribution and Its Effect on Fluid Flow in a Deltaic Sandstone, Frontier Formation, Wyoming," AAPG Bull., **86**(12), pp. 2007–2021.
[58] Bažant, Z. P., and Ohtsubo, H., 1977, "Stability Conditions for Propagation of a System of Cracks in a Brittle Solid," Mech. Res. Commun., **4**(5), pp. 353–366.
[59] Bažant, Z. P., and Ohtsubo, R., 1978, "Geothermal Heat Extraction by Water Circulation Through a Large Crack in Dry Hot Rock Mass," Int. J. Numer. Anal. Method Geomech., **2**(4), pp. 317–327.
[60] Bažant, Z. P., Ohtsubo, R., and Aoh, K., 1979, "Stability and Post-Critical Growth of a System of Cooling or Shrinkage Cracks," Int. J. Fract., **15**(5), pp. 443–456.